MID-INFRARED VIBRATIONAL SPECTRUM CHARACTERIZATION OF THE OUTER SURFACE OF *Candida albicans* BY FUNCTIONALLY ENHANCED DERIVATIVE SPECTROSCOPY **

S. L. Palencia [1,2*], A. García [1], M. Palencia [3]

[1] *Laboratory of Bacterial Pathogenicity, Department of Microbiology,*
Faculty of Biological Sciences, Universidad de Concepción, Concepción – Chile;
e-mail: sixta.palencia3004@gmail.com
[2] *Microbiology and Bioengineering Division, Mindtech Research Group (Mindtech-RG),*
Mindtech s.a.s., Cali – Colombia
[3] *Research Group in Science with Technological Applications (GI-CAT),*
Department of Chemistry, Faculty of Natural and Exact Sciences, Universidad del Valle, Cali – Colombia

    The objective of this work was to evaluate the ability of the functionally enhanced derivative spectroscopy (FEDS) algorithm to characterize the surface of microorganisms, namely, Candida albicans, by mid-IR spectroscopy and with the cellulose sensing surface technique. This work is a key stage in the study of cell-cell and cell-surface interactions between microorganisms, including the study of polymicrobial biofilms. Accordingly, C. albicans was selected as a microorganism model due to its importance in medical science and human health. Spectra were recorded in triplicate from 4000 to 500 cm^{-1} by the ATR technique. It was concluded that the FEDS transform of the mid-IR spectrum is a powerful analytical tool to improve spectral analysis by IR spectroscopy. In the particular case of C. albicans biofilms, it was observed that by FEDS, it is possible to deconvolute signals and achieve improved signal differentiation. For interpretation, serine, threonine, glycine, alanine, glutamic acid, proline, and N-acetyl-D-glucosamine units were taken as molecular models since these molecules have been described as the main components in the cell wall of C. albicans. In this way, it was found that the vibrational spectrum of C. albicans biofilms can be understood considering only the main components of the cell wall.

    Keywords: *Candida albicans, mid-IR spectrum, biofilm, FEDS transform, sensing surface.*

ИК-СПЕКТРОСКОПИЧЕСКИЙ АНАЛИЗ ВНЕШНЕЙ ПОВЕРХНОСТИ КЛЕТОЧНОЙ СТЕНКИ *Candida albicans* С ИСПОЛЬЗОВАНИЕМ МЕТОДА ФУНКЦИОНАЛЬНО-УСИЛЕННОЙ ПРОИЗВОДНОЙ

S. L. Palencia [1,2*], A. García [1], M. Palencia [3]

УДК 543.42

[1] *Университет Консепсьон, Консепсьон, Чили;*
e-mail: sixta.palencia3004@gmail.com
[2] *Исследовательская группа Mindtech (Mindtech-RG), Mindtech s.a.s., Кали, Колумбия*
[3] *Университет дель Валле, Кали, Колумбия*

    Оценена способность алгоритма функционально-усиленной производной спектроскопии (FEDS) характеризовать поверхность микроорганизмов, а именно Candida albicans, с помощью спектроскопии среднего ИК-диапазона и сенсоров на основе целлюлозы. Работа является ключевой в изучении межклеточных и клеточно-поверхностных взаимодействий микроорганизмов и включает в себя изучение полимикробных биопленок. Грибок C. albicans выбран в качестве модели микроорганизма из-за

его важности в медицинской науке и для здоровья человека. Спектры в диапазоне 4000–500 см⁻¹ за-регистрированы методом нарушенного полного отражения в трех повторениях. В случае биопленок C. albicans с помощью FEDS можно деконволюционировать сигналы и добиться их улучшенной диф-ференциации. Серин, треонин, глицин, аланин, глутаминовая кислота, пролин и N-ацетил-D-глюко-замин взяты в качестве молекулярных моделей при анализе спектров, поскольку считаются основ-ными компонентами клеточной стенки C. albicans. Показано, что колебательный спектр биопленок C. albicans можно изучать, рассматривая только основные компоненты клеточной стенки.

__Ключевые слова:__ Candida albicans, спектр среднего ИК-диапазона, биопленка, преобразование с использованием алгоритма функционально-усиленной производной спектроскопии (FEDS), чувстви-тельная поверхность.

Introduction. A biofilm is understood to be an assemblage of microbial cells that is irreversibly associ-ated with a surface and is enclosed in a matrix of primarily polysaccharide material; however, biofilms can also be constituted by non-cellular materials such as mineral crystals, corrosion particles, clay or silt parti-cles, or blood components, among others [1–4]. In addition, biofilms can colonize abiotic and biotic surfaces and proceed through distinct stages, which can be broadly categorized into reversible adhesion stages and ir-reversible cohesion stages [3, 4]. Moreover, it is also widely recognized that biofilms are an important prob-lem for human health, contributing to ~80% of hospital infections [4].

Adhesion between bacteria and surfaces can be studied by a variety of methods including scanning elec-tron microscopy (SEM), transmission electron microscopy (TEM), and fluorescence microscopy, among others [2, 5]. The main limitations in the case of SEM and TEM are the high cost of equipment, high pertur-bation of samples, and limited molecular information. Fluorescence techniques are based on 'the making' of systems that are different from those that are being studied.

This study proposes that by correctly characterizing surfaces, important information regarding microor-ganism surfaces can be obtained and directed toward multiple objectives. In particular, studying interactions between microorganisms is an important aspect in the study of pathogenicity and prevalence mechanisms. Consequently, in this study, the analysis of the microorganism surface was observed to be satisfactorily car-ried out by spectroscopic techniques since they permit obtaining molecular-level surface information. In par-ticular, the use of infrared spectroscopy in the mid-infrared (mid-IR) region is proposed by the attenuated to-tal reflectance (ATR) technique.

Mid-IR spectroscopy is based on the use of IR radiation to produce changes in vibrational states at the molecular level. In addition, this technique is characterized by being a nondestructive, fast, easy to use, and highly sensitive method for microbial analysis, as well as requiring a small sample size without complex pre-treatment procedures. Mid-IR spectroscopy is also a very useful method for determining the presence or ab-sence of functional groups, for the analysis of new molecular interactions or changes in those interactions by monitoring and examining the position, displacements, and intensity of the different IR signals [6–8], and for the monitoring of bioprocesses such as biofermentation, microbial biodegradation pathways, and bacterial biofilms on implantable devices [9–12]. However, for microbiological analysis, the main limitations of mid-IR spectroscopy are the high spectral similarity between the spectra of different microorganisms, the high overlap of signals, and the broadening of adjacent signals [6–8]. To resolve these problems, mathematical and computerized methods are usually used, with Fourier deconvolution being the most common [13–15]. However, although Fourier self-deconvolution is simple from a conceptual standpoint, its application is lim-ited by the relatively high complexity of computation, the appearance of negative intensities from calcula-tions, the high sensitivity to noise, and the appearance of 'false' signals resulting from mathematical argu-ments without physical meaning [13]. In contrast, a simple method for deconvoluting and increasing the spectral resolution of signals has been recently developed. This method is based on the transformation of a spectrum by the use of a derivative algorithm enhanced by functional transformations and has been named functionally enhanced derivative spectroscopy (FEDS) [15].

The objective of this work was to evaluate the ability of the functionally enhanced derivative spectros-copy **(**FEDS) algorithm to characterize the surface of microorganisms, namely, *Candida albicans*, through mid-IR spectroscopy analysis of artificial biofilms deposited on spectrally marked cellulose surfaces. This work is a key stage in the study, by IR spectroscopy, of cell-cell and cell-surface interactions between mi-croorganisms, including the study of polymicrobial biofilms.

Materials and methods. *Yeast strains and growing conditions.* ATCC strains of *C. albicans* were used as a model microorganism, which was supplied by the Laboratory of Bacterial Pathogenicity of Universidad de Concepción. This yeast was selected due to its importance for research on human health. The *C. albicans* strain was grown by inoculation in tryptic soy broth (TSB) (Invitrogen, Carlsbad, CA, USA) and standardized to 0.5 on the McFarland scale by absorbance measurements at 625 nm using turbidity standards prepared from a $BaCl_2$ solution (0.048 mol/L) and H_2SO_4 (0.18 mol/L). Later, subsamples of yeast were separately inoculated in Müller-Hinton agar and incubated for 24 h at 37°C. Gram staining was performed when yeast growth was observed.

Preparation of samples and recording of spectra. Artificial yeast biofilms, or biolayers, were deposited on ultrafiltration cellulose membranes that were previously modified using a spectral marker (CISM®, Mindtech s.a.s., Colombia). CISM® is a spectral marker producing a characteristic mid-IR signal at ~2268 cm^{-1}; this signal is absent in the mid-IR spectrum of yeast and, consequently, can be used to monitor background signals associated with the cellulose support.

To eliminate residual growth medium on the surface, after forming the biolayer on the support, samples were successively washed with deionized water and dried for 12 h using a laminar flow oven with the temperature controlled at 40°C. To evaluate this stage, spectra of support and blank experiments, i.e., growth medium without bacteria, were compared with the respective spectra of biofilm samples. Finally, biolayers were analyzed using an infrared spectrophotometer with ATR using a ZnSe crystal (ATR, IR-Affinity, Shimadzu Co.). Biolayers were performed in triplicate, and for each replicate, 20 spectral scans from 500 to 4000 cm^{-1} were recorded and averaged. Data were extracted in .txt file format in order to carry out the analysis using a spreadsheet.

Pretreatment of data. For each region of the spectrum being analyzed, data were autoscaled with respect to the values of the minimum and maximum absorbances ($a_{\min}$ and $a_{\max}$):

$$b_j = (a_j - a_{\min})/(a_{\max} - a_{\min}), \tag{1}$$

where a_j and b_j are the experimental absorbance in the j-position and the corresponding autoscaled absorbance, respectively. Note that the j-position can be directly correlated with the wavenumber. To avoid calculation mistakes resulting from scaling from 0 to 1 during the application of the FEDS algorithm, the zero absorbance was approximated by calculating the average value between two adjacent values of absorbance satisfying $b_{j-1} < b_j < b_{j+1}$, with $b_j = 0$. Since the derivative spectrum is strongly sensitive to the noise in the original signal, the smoothing of spectral noise was decreased by the use of an average-based spectral filter (ABSF) [15]. The ABSF is given by

$$\text{ABSF}(b_i; N = 20) = \frac{1}{3} \sum_{j}^{j+2} \left(b_j \right) \Big|_{N=1}^{N=20}. \tag{2}$$

The ABSF is the moving average with a data window of 3 and 20 cycles ($N = 20$). Thus, for each b_j, b_{j+1}, and b_{j+2}, the corresponding average value is calculated, and subsequently, this procedure is repeated N times. However, as the spectrum line function in the absorbance domain is modified by the use of Eq. (2), the same data transformation is performed on wavenumber (ν) values to correct the displacements with respect to the original spectrum (i.e., the maximum points in the original spectrum should be the same in the original and smoothed spectra) [15].

Fundamentals and calculations. For the application of the FEDS transform to the mid-IR spectrum, the spectrum is considered to be a function **z** with **z**:(ν_j, b_j). By FEDS, a new spectrum with sharper signals is obtained, but since the intensities of signals with a higher SNR are increased, the deconvolution of overlapping signals is produced. Thus, to obtain the FEDS intensities, the first step is to calculate the first-order derivative of the inverse of the normalized spectrum; therefore, the FEDS transform is a method of derivative spectroscopy applied to the inverse function of the IR spectrum. This first stage can be easily calculated by

$$\frac{d\mathbf{z}}{d\nu} = \frac{1/b_j - 1/b_{j-1}}{\nu_j - \nu_{j-1}}. \tag{3}$$

Assuming that $\nu_j - \nu_i$ is always a constant (this assumption is valid for almost all instrumental equipment), Eq. (3) is rewritten as

$$p = 1/b_j - 1/b_{j-1}, \tag{4}$$

where p denotes an auxiliary function p in order to simplify the notation (the notation p comes from the Spanish word '*primera*' alluding to the use of the first derivative). Since Eq. (4) defines positive and negative

values, the mathematical operator $1/|x|^{0.5}$ is applied, where x denotes any mathematical arguments. This operator is equal to the scale factor defined under the wavelet concept, which is used to define the general expression of the 'mother wavelet' [15]. Thus, for each b_j, a new function called function P transforms the values of function p by

$$P_j = (1 + b_j) / \sqrt{| p_j |}, \tag{5}$$

where $(1 + b_j)$ is an amplification factor for assigning a weight congruent with absorbance intensity, and P defines a new magnitude called the FEDS intensity.

At present, the FEDS transform has only been used for the quantification of water content in mixtures with organic acids, determination by spectral analysis of dimerization constants, deconvolution of the mid-infrared spectrum of quaternized poly(vinyl chloride) for the assignment of signals, and recognition of specific signals in polymers [15, 16].

Results and discussion. *Mid-IR spectrum of C. albicans biofilms.* Figure 1 shows the main signals identified in the IR spectrum of *C. albicans*. These signals have been described widely in works [7, 8, 17–24]. However, these signals do not enable obtaining specific information about the biofilm since these are common for all microorganisms. A summary of the signals and their chemical nature is shown in Table 1. Based on the above, the use of FEDS appears to be an interesting analytical tool for increasing the spectral resolution of IR spectra. To ease the FEDS analysis of the spectrum, different analysis windows were defined: 4000–3000, 3000–2500, 2500–2000, 2000–1300, and 1300–600 cm^{-1}.

TABLE 1. Assignation of Main Signals Observed in the Mid-IR Spectrum of *C. albicans* Biofilms

| Analysis window, cm^{-1}	Wavenumber, cm^{-1}	Description
3000–4000	No specified	Vibrations associated with O-H and N-H groups. It is not possible to indicate a specific signal due to the overlap. This band is affected by the presence of water, alcohols, amines, etc. [8, 15]
2500–3000	2800–3000	Vibrations associated with C-H. These vibrations can be C-H of methyl groups, methylene groups, or C-H in a ring or cyclic structure [8]
	< 2800	Though S-H vibrations are not identified these are expected in this region (usually these are very weak signals) [21]. In addition, some vibrations modes of N-H are expected in this region [21]
2000–2500	2240–2350	Vibration of NCO. This signal is not associated with the bacterial biofilm but is associated with spectral marker onto support surface [22–24]
1300–2000	1650	Amide I corresponding to C=O stretching vibration with minor contributions from out-of-phase CN stretching vibration, the CCN deformation, and the NH in-plane bending [20]
	1550	Amide II corresponding to out-of-plane combination of the NH in plane bending and the CN stretching vibration with smaller contributions from the CO in plane bending and the CC and NC stretching vibrations [20]
	1450	Amide III corresponding to the in-phase combination of NH bending and the CN stretching vibration with small contributions from the CO in plane bending and the C-C stretching vibration [20]
	1400	Symmetric stretching of carboxylate group observed in several bacteria [7, 19]
600–1300	1240	Vibration of P=O ($y1$). The assignment was based on models for DNA phosphodiester group [17, 18] and by comparison with results of other researchers with different bacteria [19]
	1050	P=O ($y2$). The assignment was based on models for DNA phosphodiester group [17, 18] and by comparison with results of other researchers with different bacteria [19]
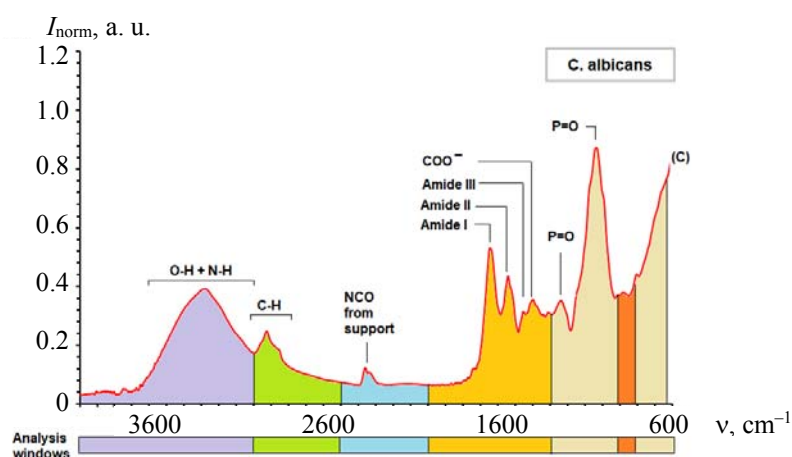
Fig. 1. Averaged IR spectrum of *C. albicans* obtained by ATR technique.

FEDS spectrum of C. albicans biofilm (4000–3000 cm⁻¹ and 3000–2500 cm⁻¹). In Figure 2, the analysis windows of the FEDS spectrum of *C. albicans* corresponding to 4000–3000 and 3000–2500 cm^{-1} are shown. Between 4000 and 3000 cm^{-1}, two signals are observed, since in this region signals associated with vibrations of O–H and N–H are expected. The first band, at 3560 cm^{-1}, was associated with O–H groups, whereas the second band, at 3281 cm^{-1}, was associated with N–H groups due to the higher electronegativity of oxygen atoms than of nitrogen atoms. Both signals can be explained by the presence of peptidoglycan on the surface of *C. albicans*, which is constituted by disaccharides and peptides with O–H groups and N–H units on their structures [25].
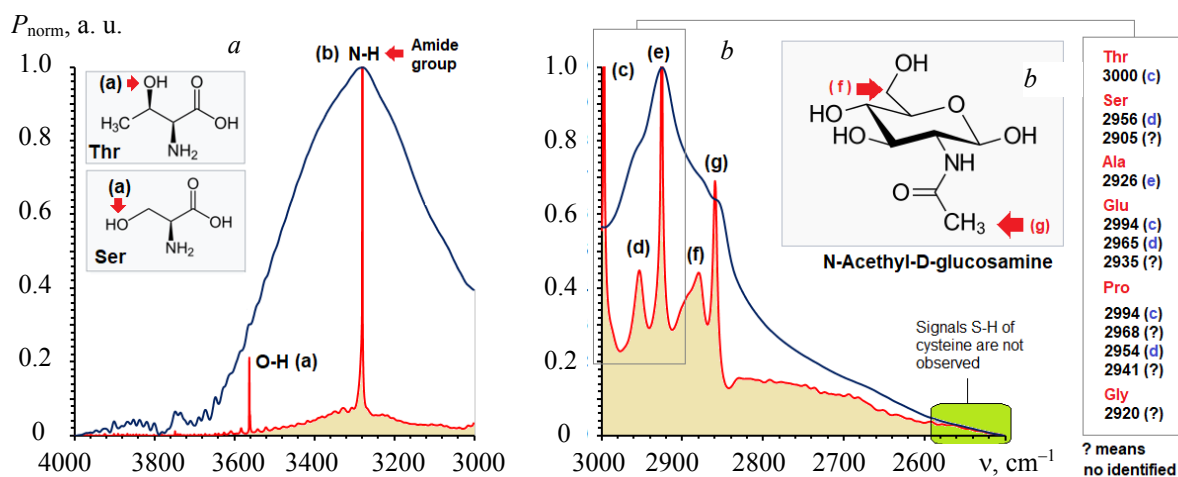

Fig. 2. FEDS transform of IR spectrum of *C. albicans* obtained by ATR technique:
(a) 3000–4000 cm^{-1} and (b) 2500–3000 cm^{-1}.

The signal associated with O–H is expected because approximately 80 to 90 % of the cell wall of *C. albicans* is constituted by carbohydrates, described by three types of polysaccharides: (i) branched polymers of glucose containing β-1,3 and β-1,6 linkages (β-glucans), corresponding to 20–40% of the dry weight of the cell wall, (ii) unbranched polymers of N-acetyl-D-glucosamine (NAcGlc) containing β-1,4 bonds (chitin), corresponding to 1–2% of the dry weight of the cell wall, and (iii) polymers of mannose (mannan) covalently associated with proteins (glyco[manno]proteins) [25–27].

It is important to note that the outer layer of the cell wall of *C. albicans* is mainly composed of mannoproteins [27], which would explain the signal associated with the N–H and O–H vibrations since the amount of chitin is very small. Whereas chitin is 1–2% of the cell wall, mannoproteins correspond to approximately

40% of the cell wall of *C. albicans* [26, 27], and given that these proteins are localized in the external layer of yeasts, they are expected to show a better interaction with IR light during ATR analysis. From the above facts and considering the main amino acid composition of the cell wall of *C. albicans* [28], where three fractions of amino acids are described, it is concluded that the O–H signals could be mainly associated with side chains of threonine and serine, whereas the signal N–H is mainly associated with N–H vibrations of amide groups of peptide chains formed by threonine, serine, glutamic acid, proline, glycine, and alanine (Table 2; in addition, respective structures are shown in Fig. 3).

TABLE 2. Main Amino Acids Constituting the Cell Wall of *Candida albicans*

Fraction	Protein content, %	Main amino acids	Content of amino acid, %	Main no-peptide structural units on the chains of amino acids			
A	>50	Threonine (Thr)	21.1	$-CH_2$	$-CH_3$	-OH	–
		Serine (Ser)	13.3	$-CH_2$	-OH	–	–
		Glutamic acid (Glu)	12.3	$-CH_2$	-OH	C=O	COO-
		Proline (Pro)	12.2	-CH	$-CH_2$	–	–
		Glycine (Gly)	6.7	$-CH_2$	–	–	–
B	>90	Serine (Ser)	20.6	$-CH_2$	-OH	–	–
		Threonine (Thr)	15.5	$-CH_2$	$-CH_3$	-OH	–
		Alanine (Ala)	12.4	$-CH_3$	–	–	–
		Glutamic acid (Glu)	9.8	$-CH_2$	-OH	C=O	COO-
		Proline (Pro)	7.6	-CH	$-CH_2$	–	–
C	~25	Serine (Ser)	15.2	$-CH_2$	-OH	–	–
		Alanine (Ala)	13.9	$-CH_3$	–	–	–
		Glycine (Gly)	11.7	$-CH_2$	–	–	–
		Glutamic acid (Glu)	9.2	$-CH_2$	-OH	C=O	COO-
		Threonine (Thr)	8.1	$-CH_2$	$-CH_3$	-OH	–

N o t e. Fraction A, B, and C corresponding to 24, 10, and 70–80 % of wall cell, respectively [28].
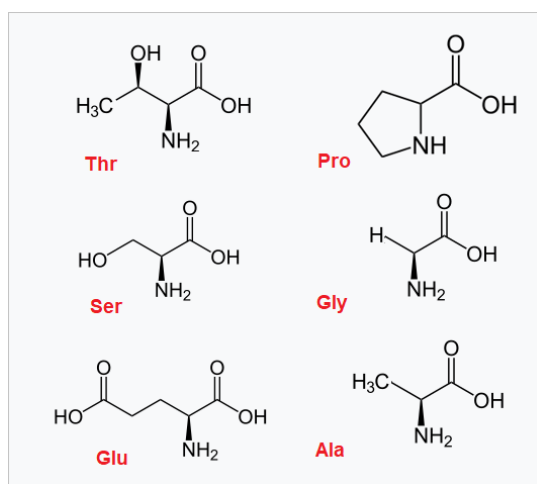

Fig. 3. Structure of main amino acids forming the cell wall of *C. albicans*.

Note that by computational calculations based on density functional theory (DFT), the O–H signal for serine in aqueous solution is expected at 3500 cm^{-1}, but it is observed at 3529 cm^{-1}; however, by the formation of hydrogen bonds, this signal is displaced to 3556 cm^{-1} [29]. On the other hand, by DFT, the O–H signal for threonine in aqueous solution is expected at 3560 cm^{-1} due to the formation of hydrogen bonds [29]. These results are consistent with those obtained by the FEDS transform, which situates the signal at 3560 cm^{-1}. Note that this signal is not observed in the IR spectra of *C. albicans*, and can only be identified by FEDS, demonstrating the ability of FEDS to deconvolute the IR spectrum and visualize overlapping signals. In addition, the analytical power of FEDS as a tool for data analysis is evidenced by its ability to associate this specific signal, in conjunction with theoretical and computational calculations, with the O–H side

chains of amino acids on the peptide chain, suggesting that the same analysis could be performed with the theoretical spectra of monomers of the respective polysaccharides. Thus, the basic structural units identified in the cell wall of *C. albicans*, i.e., glucose (glucans), N-acetyl-D-glucosamine (chitin), and mannose (mannan), can be used in conjunction with DFT to facilitate the assignment of signals obtained by FEDS [26–28]; for example, for sucrose, which is a disaccharide constituted by glucose and fructose units, the O–H signal on fructose is expected at 3559 cm^{-1}, whereas for glucose, it is expected at 3382 cm^{-1} [30]. Note that peptidoglycans of *C. albicans* are not formed by fructose units but by glucose units, and consequently, the important signal for our analysis is at 3382 cm^{-1}. For mannose, the experimental spectrum shows that the signals of O–H vibrations are between 3000 and 3500 cm^{-1} [31] and from computational data are at 3742, 3740, 3736, 3603, 3305, and 3249 cm^{-1} [32]. Other authors describe three vibrations associated with O–H stretching vibrations of mannan I or poly-β-D(1-4)mannose: 3497, 3462, and 3365 cm^{-1} [33]. Finally, for N-acetyl-D-glucosamine, the signals associated with O–H stretching vibrations are expected at 3458, 3391, 3376, 3326, and 3197 cm^{-1} [34]. These results suggest that by the use of FEDS, signals of O–H vibrations produced by peptides can be differentiated from signals of O–H vibrations produced by polysaccharides constituting peptidoglycans.

The signal at 2280 cm^{-1}, identified by FEDS and easily visualized in the IR spectrum, is associated with N–H stretching vibrations. This signal is directly related to amide groups (–CONH–) resulting from the linking of amino acids to form polypeptides in the outer layer of the wall cell.

On the other hand, signals observed in the analysis window from 3000–2500 cm^{-1} are not important because they are present in many organic molecules. Considering that the main signals are associated with the outer layer of the cell wall, from vibrational analysis by computational techniques, signals associated with the side chains of the main amino acids described in Table 2 were used to achieve a coherent assignment of signals.

Thus, for threonine, one signal at 3000 cm^{-1} has been described and associated with C–H bonds in CH_3, whereas for serine, three signals have been described at 3004 cm^{-1} (stretching), 2956 cm^{-1} (asymmetric stretching), and 2905 cm^{-1} (symmetric stretching) associated with C–H bonds in CH_2 [29]. For alanine, asymmetric C–H stretching in CH_3 has been experimentally observed at 2926 cm^{-1} and for glutamic acid, a signal associated with C–H stretching in CH_2 is observed at 2994 cm^{-1}; with CH_2 asymmetric stretching, at 2965 cm^{-1}; and with CH_2 symmetric stretching, at 2935 cm^{-1} [35]. For proline, antisymmetric stretching vibrations associated with CH_2 are observed at 2994 and 2968 cm^{-1}, whereas symmetric stretching vibrations are observed at 2954 and 2941 cm^{-1} [36]. For glycine, two signals associated with asymmetric stretching vibrations at 3084 cm^{-1} and symmetric stretching vibrations at 2920 cm^{-1} have been observed in the IR spectrum [4]. Consequently, in the analysis window between 2500 and 3000 cm^{-1}, approximately 11 signals associated with C–H vibrations in the CH_2 and CH_3 groups are expected. In this way, the signals described in Fig. 2 as **c**, **d**, and **e** can be associated with vibrational modes of C–H in CH_2 and CH_3 of the main amino acids forming the outer layer of the cell wall of *C. albicans*.

On the other hand, during the evaluation of FTIR spectroscopy as a potential tool for the study of structural modifications of *C. albicans*, signals associated with vibrations of CH_2 from lipids have been described at 2851, 2873, 2924, and 2960 cm^{-1}, whereas one signal associated with C–H bonds from methyl groups is assigned at 2893 cm^{-1} [37]; however, this assignment was not considered due to the low content of lipids in the cell wall of *C. albicans* (1–7%) [26].

By analysis of the FTIR spectra of N-acetyl-D-glucosamine (NAcGlc), two signals have been described at 2829 and 2893 cm^{-1} in the solid state and one at 2895 cm^{-1} in aqueous solution; however, by theoretical calculations, these signals are expected to be 2889 cm^{-1} for C–H groups and 2859 cm^{-1} for CH_2 [34]. It is known that (i) 80–90% of the cell wall of *C. albicans* is composed of carbohydrates, including NAcGlc; that (ii) mannose polymers (mannan), which do not exist in a free form but are found in covalent association with proteins (mannoproteins), represent approximately 40% of the total cell wall polysaccharide corresponding to the main material of the cell wall matrix of *C. albicans*; and that (iii) mannose polymers are linked to the protein moiety through asparagine by N-glycosidic bonds through two NAcGlc units [26]; thus, it is concluded that the signals *f* and *g* can be associated with signals from NAcGlc, and hence, the signal at 2880 cm^{-1} is assigned to the C–H bonds in the CH_3 group of NAcGlc (**f**), whereas the signal at 2860 cm^{-1} is assigned to C–H bonds in the CH_2 groups (*g*) of NAcGlc.

In addition, important conclusions can be made considering the signals that do not appear in the spectrum. For example, a stretching vibration signal associated with the C–H bond in the phenyl ring of phenylalanine is expected to appear at 2918 cm^{-1} [35], and for cysteine, three signals are expected at 2543, 2545,

and 2552 cm^{-1} associated with the vibrational modes of the S–H bond [21]. The above is consistent with the low content of phenylalanine (fractions *A*, *B*, and *C*: between 3.5 and 4.6%) and cysteine (fraction *A*: 0.3 %; fractions *B* and *C*: not identified) described in previous publications [28].

FEDS spectrum of C. albicans biofilm (2000–2500 cm^{-1}). Figure 4 shows the FEDS transform of the IR spectrum of *C. albicans* in the region from 2000–2500 cm^{-1}. In this region, signals are not usually found in samples of living organisms; in addition, this area is characterized because very few functional groups have infrared signals in this region. The main and more characteristic signal corresponds to the isocyanate group (–NCO), which was used as a spectral marker of the surface of the cellulose support. Note that for methyl isocyanate, the stretching signal associated with –NCO has been identified at 2288 cm^{-1} [38], whereas for phenyl isocyanate, the same signal is described at 2285 cm^{-1} (asymmetric stretching), but with two additional signals with lower intensity at 2340 and 2370 cm^{-1} corresponding to non-fundamental signals [39]. The results obtained by FEDS are consistent with the signals from phenyl isocyanate since the marker used was based on MDI. The signals identified were at 2365 (*h*), 2340 (*i*), and 2278 cm^{-1} (*j*).
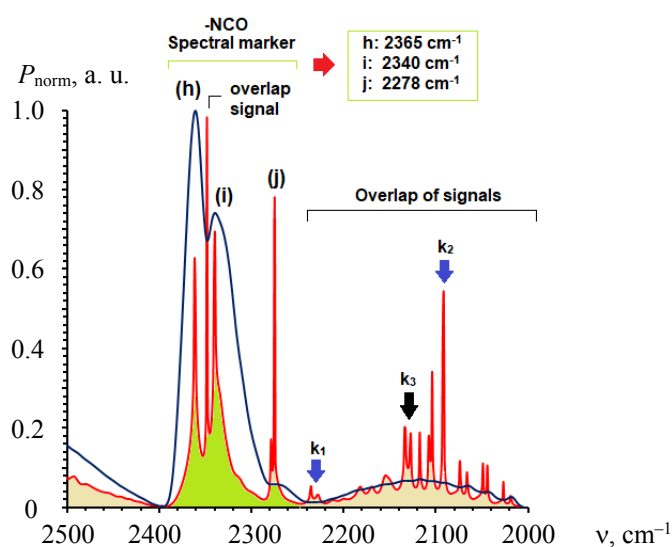

Fig. 4. FEDS spectrum of *C. albicans* biofilms between 2500–2000 cm^{-1}.

Other non-fundamental signals associated with symmetric stretching vibrations of –NCO (expected at 1448 cm^{-1}) have been reported at 2207 and 2090 cm^{-1} (these signals were identified as k_1 and k_2, respectively) [39]. However, in this region, one combined signal appears at 2128 cm^{-1} (k_3), which can change depending on the molecular ordering of water molecules [40].

FEDS spectrum of C. albicans biofilm (1300–2000 cm^{-1}). Figure 5 shows the FEDS transform of the IR spectrum of *C. albicans* in the region from 2000–1300 cm^{-1}. As expected, the complexity of the FEDS spectrum is increased in comparison with that of the IR spectrum, which is the typical observation in derivative spectroscopy. For interpretation, a direct comparison with the IR spectrum was performed, and as a result of this procedure, four signals were identified, namely, Am-1, Am-2, Am-3 and -COO$^-$, which were previously explained in Table 1. However, by analyzing the relative-minimum point in the line function of the spectrum, it is possible to identify eight overlapping signals, which is reasonable because the number of signals in this region is significantly increased. These signals were named from k_4 to k_{11} in order to continue with the numbering of previously identified overlapping signals. In addition, signals with FEDS intensities lower than 2% were not taken into consideration since their contribution is very small (signals between 1800 and 2000 cm^{-1}). Thus, 17 new signals were obtained from the FEDS transform for this analysis window, which were named from *d*1 to *d*13.

Note that the assignment of signals is very difficult due to the nature of the sample, the appearance of new signals that were previously not identified in the IR spectrum, and the lack of available information about the FEDS transform and IR spectra of *C. albicans*. Therefore, to assign the signals, the signals of the previously identified main components constituting the cell wall of *C. albicans* were used to perform a correlation analysis. Thus, the set of signals described for individual molecules in the analysis windows were

grouped with a variation of ± 5 cm^{-1} and compared with signals observed from the FEDS spectrum (Table 3). By correlation analysis, signals $d1$, $d2$, $d3$, $d5$, $d6$, $d8$, and $d10$ were not identified. On the other hand, many of these signals are common for many organic compounds, and from an analytical point of view, these are not important. In particular, signal k_8, which is identified as an overlapping signal, is seen to exhibit an adequate correlation with the vibration of C–O–H, and therefore, it is not completely clear if there is some hidden signal since this signal is coherent with the presence of the –OH group on the side chain of threonine, which is an important component of the cell wall of *C. albicans*. On the other hand, three signals are identified to be very important since these are associated only with NAcGlu units: $d7$ (1550 cm^{-1}), $d12$ (1435 cm^{-1}), and $d14$ (1380 cm^{-1}).
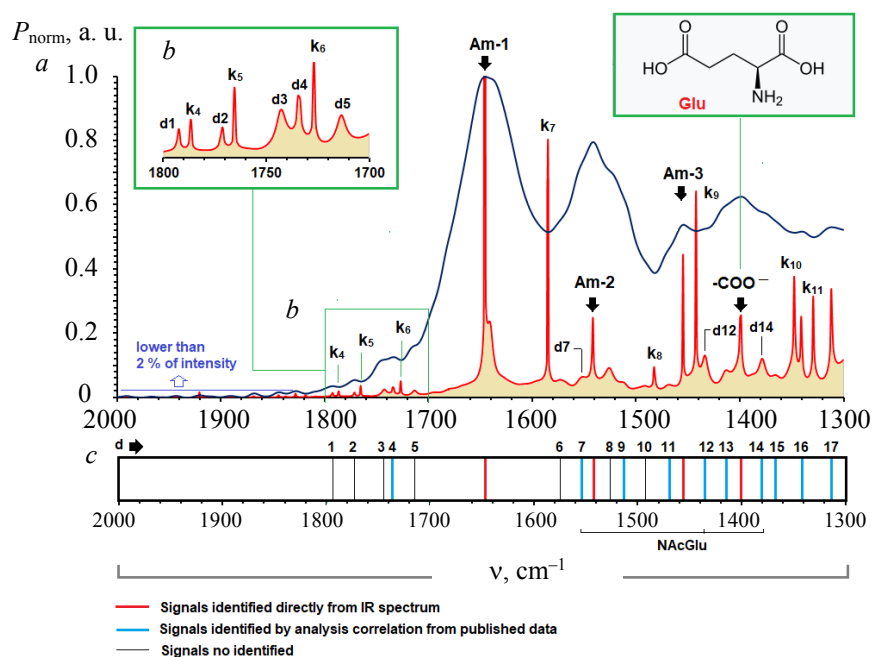

Fig. 5. a) FEDS spectrum of *C. albicans* biofilms between 2000–1300 cm^{-1}; b) magnification of region between 1800 and 1700 cm^{-1}; c) signal discontinuous patterns for range under study.

TABLE 3. Analysis of Correlation of Signals Described for Main Components
of Cell Wall of *C. albicans* [4, 29, 34–36]

Signal	Wavenumber for main components of *C. albicans*, cm^{-1}							FEDS	Id. Code
	Ala	Gly	Ser	Thr	Glu	Pro	NacGlu		
No identified								1794	$d1$
C=O (st)				1781					
No identified								1772	$d2$
No identified								1743	$d3$
NH (b)		1730						1735	$d4$
No identified								1715	$d5$
C=O (st) + others		1703							
C=O (st)						1687			
COO (v)				1640	1635				
CH (b) + CH$_2$ (b)									
C=O (v)							1627		
NH$_2$ (sc)		1610	1610						
NH$_2$ (b)	1595			1596					
No identified								1570	$d6$
NH (v)							1550	1550	$d7$

Continue Table 3

Signal	Wavenumber for main components of *C. albicans*, cm^{-1}							FEDS	Id. Code
	Ala	Gly	Ser	Thr	Glu	Pro	NacGlu		
NH$_2$ (b)						1542			
No identified								1525	*d*8
CH$_2$ (b) CH$_2$ (b) + OH (b)		1504	1509					1510	*d*9
No identified								1490	*d*10
C-O-H (v)			1481					1483	*k*8
CH$_2$ (r), CH$_2$ (b) CN (st), OH (v)		1468				1472 1465	1473	1470	*d*11
CH$_2$ (b) CH$_3$ (v)			1452			1457 1448	1452		
CH (v), OH (v)							1430	1435	*d*12
OH (b), C-O-H N-C-H (v) CH$_2$ (sc) CH (b-in-p)		1412 1410	1411	1415	1405			1415	*d*13
CO (st) + CH$_2$ (t) CH (v), OH (v)					1386		1388		
CH (v), OH (v)						1377		1380	*d*14
CH$_2$ (w) C-OH (st) NH$_2$ (sc)	1354					1361 1357		1365	*d*15
CH (v)						1348			
NH (b) + CN (b) C-C-H (v) N-C-H (v) H-C-O (v)		1341		1340				1342	*d*16
CO (st) + CO (st) CH (st) + C-C (v)		1334			1337				
CH$_2$ (d-in-p) CH (v), CH$_2$ (v)						1325	1328		
C-O-H (v) CH$_2$ (w)			1312			1314		1312	*d*17
CH$_2$ (t) CH$_2$ (d-out-p)					1301	1302			

N o t e. Stretching (st), bending (b), scissoring (sc), bending in-plane (b-in-p), torsion (t), no-specified vibration (v), rocking (r), wagging (w), deformation (d), deformation in-plane (d-in-p), deformation out-plane (d-out-p); Gray row shows signals obtained by FEDS that can be correlated with at least one signal described in previous publications. Red letter indicates signals that could not be identified by this procedure.
Correlation of signals was performed with a tolerance of ±5. Analysis window between 1300 and 2000 cm^{-1}. Shaded rows correspond to signals with adequate correlation.

Figure 6 shows the FEDS transform of the IR spectrum of *C. albicans* in the region from 1300–600 cm^{-1}. It can be seen that complexity of the FEDS spectrum in this region increases compared with that of the IR spectrum. By a procedure analogous to that applied for the region from 2000–1300 cm^{-1}, the signal assignment was based on available information of IR vibrations of main components of the cell wall of *C. albicans* and by direct comparison with the IR spectrum. Thus, by direct comparison, two signals associated with P=O bonds were identified (named *y*1 and *y*2). On the other hand, from correlation analysis (Table 4), some signals were not identified (*E*10, *E*11, *E*16, *E*20, *E*23, and *E*24), and others were correlated with multiple vibrations associated with different groups of amino acids and NAcGlu; therefore, an exact assignment was not possible. However, four signals correlated only with NAcGlu, permitting these signals to be associated with this specific component; thus, signals *E*7 (1000 cm^{-1}), *E*15 (830 cm^{-1}), *E*17 (780 cm^{-1}), and *E*25 (630 cm^{-1}) could be used to monitor the cell wall of *C. albicans*. However, the signal *E*12 correlated only with one amino acid, Glu, and, as a consequence, this signal emerges as an important candidate

for monitoring glutamic acid in this type of biofilm; however, specific studies should be focused in this direction.
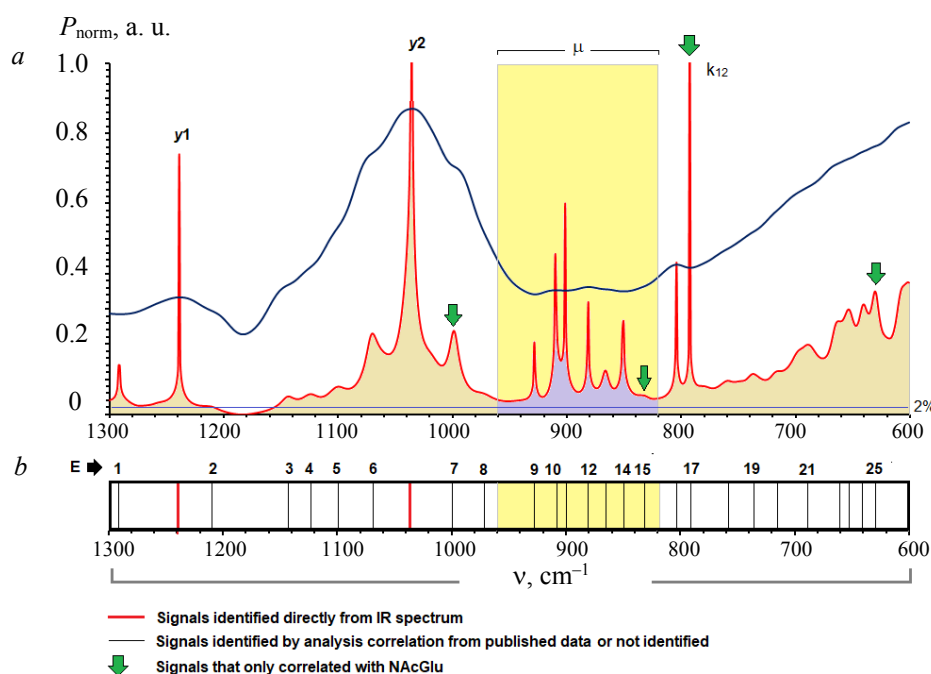

Fig. 6. a) FEDS spectrum of *C. albicans* biofilms between 1300–600 cm^{-1};
b) signal discontinuous patterns for range under study.

TABLE 4. Analysis of Correlation of Signals Described for Main Components
of Cell Wall of *C. albicans* [4, 29, 34–36]

Signal	Wavenumber for main components of *C. albicans*, cm^{-1}							FEDS	Id. code
	Ala	Gly	Ser	Thr	Glu	Pro	NAcGlu		
CH (v), OH (v), CH$_2$ (d)		1296					1290	1292	E1
CH$_2$ (t), CH$_2$ (t) + NH (b-in-p)				1279	1274				
CH (v), CN (v), NH (v)							1261		
CH (v), OH (v)				1250		1244	1248		
C-N (st) ring, H-C-C (v)									
CH (v), CH (d)						1201	1206	1210	E2
C-C-H (v)					1193				
NH$_2$ (r)						1164			
CH$_2$ (t), CH$_2$ (b) + CH (b) + NH$_2$ (b)	1149					1147		1143	E3
CO (v), CC (v), OH (b) + CH$_2$ (t) + CN (st), NH (v), H-C-C (v)			1134		1139		1136		
CC (v), CH$_2$ (v), CO (v), CN (v), OH (b-in-p)					1124		1127	1123	E4
CC (st) + CH (b) + NH (b)	1114								
CC (v), CO (v), CN (st) + OH (b-in-p)				1111	1108		1106	1112	
CH$_2$ (r), C-C (st)					1092	1093		1099	E5
CC (v), CO (v), NH (v), H-C-C (v)			1086				1088		

Continue Table 4

Signal	Wavenumber for main components of *C. albicans*, cm^{-1}							FEDS	Id. code
	Ala	Gly	Ser	Thr	Glu	Pro	NAcGlu		
N-C (st)						1079		1070	*E6*
CO (v), C-C (st) ring, CC (v), CN (v)			1057			1048	1053		
CH$_3$ (v), CO (v), CC (v)							999	1000	*E7*
C-C (st) ring						983			
CH$_3$ (v), C=O (v), CC (v)			976				973	970	*E8*
N-C-C (b)		936							
CN (v), CO (v), CC (v), CH (v), C-C (st) ring			924			924	927	929	*E9*
C-C (r), CNH (b)	918					917			
								908	*E10*
								900	*E11*
NH$_2$ (t) + CH$_2$ (t)		893							
CC (st) + CO (st)					886			882	*E12*
C-N (st) ring, CH$_2$ (r)						874			
CN (v), CO (v), CC (v), CH (v)			865				862	866	*E13*
N-C (v), CN (st) + CC (st)	850		852					850	*E14*
C-C (st)							824	830	*E15*
HOCC (b-out-p) + CH$_2$ (r)					814				
								803	*E16*
CO (v), CC (v)							787	780	*E17*
C=O (r) out-of-plane, N-C-C (v), C-C (v), HNC (b) + CCH (b)	769			772		771			
C=O (r) for carboxyl, CH$_2$ (r)					754	757		759	*E18*
O-C-O (v)				743				738	*E19*
CO (v)							727		
								715	*E20*
CO (v), NH$_2$ (b)		698					704		
CN (v), C=O (v), NH (v), COOH (b)						687	687	690	*E21*
C=O (r) ureide, HOCC (b-out-p)					668	666			
C=O··· H$_2$O			661					660	*E22*
								655	*E23*
NH$_2$ (b-out-plane), CCC (b) + COO (b)	646				646				
								640	*E24*
CO (v), C=O (v), CC (v)							625	630	*E25*
COOH (b-in-p)					612				
OH (d-out-p), COOH (b) + NCCO (b)		607				608			

N o t e. Stretching (st), bending (b), scissoring (sc), bending in-plane (b-in-p), torsion (t), no-specified vibration (v), rocking (r), wagging (w), deformation (d), deformation in-plane (d-in-p), deformation out-plane (d-out-p); Gray row shows signals obtained by FEDS that can be correlated with at least one signal described in previous publications. Red letter indicates signals that could not be identified by this procedure.

Correlation of signals was performed with a tolerance of ±5 to ±8. Analysis window between 600 and 1300 cm^{-1}. Shaded rows correspond to signals with adequate correlation.

A summary of the FEDS characterization of *C. albicans* biofilm in the mid-IR spectral range (4000–600 cm^{-1}) is shown in Table 5.

TABLE 5. Summary of Characterization by FEDS of *C. albicans* Biofilm (signals associated with overlap and signals that were not identified are omitted)

Analysis window, cm^{-1}	Wavenumber, cm^{-1}	Signal ID	Description
3000–4000	3560	*a*	Stretching of O–H. It is assigned to correspond to hydroxyls on amino acid structure (Thr and Ser)
	3280	*b*	Stretching of N–H. It is assigned to correspond to link in the peptide bond of polypeptides in the outer layer of cell wall
2500–4000	3000	*c*	C–H in CH_2 and CH_3 on the side chains of amino acids
	2950	*d*	C–H in CH_2 and CH_3 on the side chains of amino acids
	2925	*e*	C–H in CH_2 and CH_3 on the side chains of amino acids
	2880	*f*	C–H in CH_3 on the side chains of NAcGlc
	2860	*g*	C–H in CH_2 on the side chains of NAcGlc
2000–2500	2365	*h*	Asymmetric stretching of -NCO
	2340	*i*	Non-fundamental vibration of asymmetric stretching of -NCO
	2278	*j*	Non-fundamental vibration of asymmetric stretching of -NCO
	2207	k_1	Non-fundamental vibration of symmetric stretching of -NCO
	2090	k_2	Non-fundamental vibration of symmetric stretching of -NCO
	2128	k_3	Combination signal of liquid water (high overlap of signals)
1300–2000	1735	*d4*	NH bending from Gly
	1550	*d7*	Vibration of N-H
	1510	*d9*	CH_2 bending and combination of CH_2 bending + OH bending
	1483	k_8	Overlap signal. Also, it could be associated with -OH on Thr
	1470	*d11*	Multiple vibrations CH_2, CN and OH
	1435	*d12*	CH and OH on NAcGlu
	1415	*d13*	Multiple vibrations CH_2, CH and N-C-H
	1380	*d14*	CH and OH vibrations associated with NAcGlu
	1365	*d15*	CH_2 vibration in some amino acids (Ala and Pro)
	1342	*d16*	NH + CN bending, vibrations of C-C-H, N-C-H and H-C-O
	1312	*d17*	vibrations of C-O-H and CH_2
600–1300	1292	*E1*	Many structural contributions from amino acids and NAcGlu
	1238	*y1*	Vibration associated with P=O
	1210	*E2*	Many structural contributions from amino acids and NAcGlu
	1143	*E3*	Many structural contributions from amino acids and NAcGlu
	1123	*E4*	Many structural contributions from amino acids and NAcGlu
	1099	*E5*	Many structural contributions from amino acids and NAcGlu
	1070	*E6*	Many structural contributions from amino acids and NAcGlu
	1035	*y2*	Vibration associated with P=O
	1000	*E7*	Signal correlating only with NAcGlu associated with CH_3, CO and CC
	970	*E8*	Many structural contributions from amino acids and NAcGlu
	929	*E9*	Many structural contributions from amino acids and NAcGlu
	882	*E12*	Many structural contributions from amino acids and NAcGlu
	866	*E13*	Many structural contributions from amino acids and NAcGlu
	850	*E14*	Many structural contributions from amino acids and NAcGlu
	830	*E15*	Signal correlating only with NAcGlu associated with CC
	780	*E17*	Signal correlating only with NAcGlu associated with CO and CC
	759	*E18*	Many structural contributions from amino acids and NAcGlu
	738	*E19*	Many structural contributions from amino acids and NAcGlu
	690	*E21*	Many structural contributions from amino acids and NAcGlu
	660	*E22*	Many structural contributions from amino acids and NAcGlu
	630	*E25*	Signal correlating only with NAcGlu associated with C=O, CO and CC

Conclusions. The FEDS transform of the mid-IR spectrum is a powerful analytical tool for improving the analysis of IR spectra. For correct application of the technique, a minimum amount of noise is required in the working spectra; in addition, reproducibility should be ensured by the implementation of standardized protocols and the use of an appropriate number of samples.

On the other hand, the results obtained by FEDS demonstrate the capacity of this technique for improving the analysis of mid-IR spectra of microorganisms. In the particular case of *C. albicans* biofilms, it was observed that by FEDS, the deconvolution of signals is possible, permitting better signal differentiation. In this way, it was evidenced that the vibrational spectrum of *C. albicans* biofilms can be understood by considering only the main components of the yeast cell wall, and therefore, it is concluded that good results in the signal assignment during spectral characterization of the *C. albicans* surface can be obtained from IR spectra of individual components of the cell wall (where Ser, Thr, Gly, Ala, Glu, Pro, and NAcGlu units could be taken as molecular models for the signal analyses).

REFERENCES

1. J. M. Hornby, E. C. Jensen, A. D. Lisec, J. J. Tasto, B. Jahnke, R. Shoemaker, P. Dussault, K. W. Nickerson, *Appl. Environ. Microbiol.*, **67**, 2982–2992 (2001).
2. H. H. Tuson, D. B. Weibel, *Soft Matter.*, **9**, 4368–4380 (2013).
3. C. R. Arciola, D. Campoccia, G. D. Ehrlich, L. Montanaro, *Adv. Exp. Med. Biol.*, **830**, 29–46 (2015).
4. A. Kumar, A. Alam, M. Rani, N. Z. Ehtesham, S. E. Hasnain, *Int. J. Med. Microbiol.*, **307**, 481–489 (2017).
5. A. Elbourne, J. Chapman, A. Gelmi, D. Cozzolino, R. J. Crawford, V. K. Truong. *J. Colloid Interf. Sci.*, **546**, 192–210 (2019).
6. A. Alvarez-Ordoñez, D. Mouwen, M. Lopez, M. Prieto. *J. Microbiol. Methods*, **84**, 369–378 (2006).
7. J. Ojeda, M. Dittrich, *Microbiol Systems Biology: Methods and Protocols, Methods in Molecular Biology*, Springer Science (2012).
8. J. Prakash, S. Kar, C. Lin, C. Y. Chen, C. F. Chang, J. S. Jean, T. R. Kulp, *Spectrochim. Acta A: Mol. Biomol. Spectrosc.*, **116**, 478–484 (2013).
9. M. Dadd, D. Sharp, A. Pettman, C. Knowles, *J. Microbiol. Methods.*, **41**, 69–75 (2000).
10. W. Huang, D. Hopper, R. Goodacre, M. Beckmann, A. Singer, J. Draper, *J. Microbiol. Methods*, **67**, 273–280 (2006).
11. Z. Khatoon, C. McTiernan, E. Suuronen, T. F. Mah, E. Alarcon, *Heliyon*, **4**, e01067 (2018).
12. D. Singhalage, G. Seneviratne, S. Madawala, I. Manawasinghe, *Ceylon J. Sci.*, **47**, 77–83 (2018).
13. W. Friesen, K. Michaelian, *Appl. Spectrosc.*, **45**, 50–56 (1991).
14. T. Vazhnova, D. Lukyanov, *Anal. Chem.*, **85**, 11291–11296 (2013).
15. M. Palencia, *J. Adv. Res.*, **14**, 53–62 (2018).
16. M. Palencia, T. Lerma, N. Afanasjeva, *Eur. Polym. J.*, **115**, 212–220 (2019).
17. Y. Guan, C. J. Wurrey, G. J. Thomas, *Biophys. J.*, **66**, 225–235 (1994).
18. Y. Guan, G. J. Thomas, *Biopolymers*, **39**, 813–835 (1996).
19. W. Jiang, A. Saxena, B. Song, B. B. Ward, T. J. Beveridge, S. Myneni. *Langmuir*, **20**, 11433–11442 (2004).
20. A. Barth, *Biochim. Biophys. Acta*, **1767**, 1073–1101 (2007).
21. S. Parker, *Chem. Phys.*, **424**, 75–79 (2013).
22. T. A. Lerma, S. Collazos, A. Cordoba, *J. Sci. Technol. Appl.*, **1**, 30–38 (2016).
23. M. Palencia, T. A. Lerma, A. Cordoba, *J. Sci. Technol. Appl.*, **1**, 39–52 (2016).
24. N. Arbelaez, T. A. Lerma, A. Cordoba, *J. Sci. Technol. Appl.*, **2**, 75–83 (2017).
25. W. Volmer, D. Blanot, M. A. De Pedro, *FEMS Microbiol. Rev.*, **32**, 149–167 (2008).
26. W. Lajean, J. L. López–Ribot, M. Casanova, D. Gozalbo, J. P. Martínez, *Microbiol. Mol. Biol. Rev.*, **62**, 130–180 (1998).
27. E. Reyna-Beltran, C. I. Bazan, M. Iranzo, S. Mormeneo, J. P. Luna-Arias, The Cell Wall of Candida albicans: A Proteomics View, doi:10.5772/intechopen.82348 (2019).
28. J. Ruiz-Herrera, S. Mormeneo, P. Vanaclocha, J. Font-de-Mora, M. Iranzo, I. Puertes, R. Sentandreu, *Microbiol.*, **140**, 1513–1523 (1994).
29. W. Nsangou, *Comput. Theor. Chem.*, **966**, 364–374 (2011).
30. E. Wiercigroch, E. Szafraniec, K. Czamara, M. Z. Pacia, K. Majzner, K. Kochan, A. Kaczor, K. Baranska, K. Malek, *Spectrochim. Acta A: Mol. Biomol. Spectrosc.*, **185**, 317–335 (2017).

31. H. A. Wells, R. H. Atalla, *J. Mol. Struct.*, **224**, 385–424 (1990).

32. M. W. Ellzy, *Computational and Experimental Studies Using Absorption Spectroscopy and Vibrational Circular Dischroism. Thesis*, Drexel University, 1–333 (2006).

33. I. Nieduszynsky, R. H. Marchessault, *Can. J. Chem.*, **50**, 2130–2138 (1972).

34. A. Kovacs, B. Nyerges, V. Izvekov, *J. Phys. Chem.*, **112**, 5728–5735 (2008).

35. M. E. Mohamed, A. M. A. Mohammed, *Int. Lett. Chem., Phys. Astron.*, **10**, 1–17 (2013).

36. L. E. Fernández, G. E. Delgado, L. V. Maturano, R. M. Tótaro, E. L. Varetti, *J. Mol. Struct.*, **1168**, 84–91 (2018).

37. I. Adt, D. Toubas, J. M. Pinon, M. Manfait, G. D. Sockalingum, *Arch. Microbiol.*, **185**, 277–285 (2006).

38. R. P. Hirschmann, R. N. Kniseley, A. Fassel, *Spectrochim. Acta*, **21**, 2125–2133 (1965).

39. C. V. Stephenson, W. C. Coburn, W. S. Wilcox, *Spectrochim. Acta*, **17**, 933–946 (1961).

40. F. O. Libnau, O. M. Kvalheim, A. A. Christy, J. Toft, *Vibr. Spectrosc.*, **7**, 243–254 (1994).